Journal of Clinical Chemistry and Laboratory Medicine

Chen et al., J Clin Chem Lab Med 2018, 1:2

Research Article Open Access

Effects of Dibutyl Phthalate and Di-(2-ethylhexyl) Phthalate with their Metabolites on *CYP2C9*1* and *CYP2C19*1* Activities *In vitro*

Bingbing Chen[1*], Xiaoxia Hu[2], Xiang Zhen[1] and Guo-Xin Hu[1*]

[1]*Department of Pharmacology, School of Pharmacy, Wenzhou Medical University, Wenzhou, Zhejiang, China*

[2]*Department of Pharmacy, Jinhua Central Hospital, Jinhua, Zhejiang, China*

[*]***Corresponding authors:*** *Bingbing Chen, Department of Pharmacology, School of Pharmacy, Wenzhou Medical University, Wenzhou 325035, China, Tel: +86-577-8678-9710; Fax: +86-577-8668-9983; E-mail: bb55332@163.com*

Guo-xin Hu, Department of Pharmacology, School of Pharmacy, Wenzhou Medical University, Wenzhou 325035, China, E-mail: hgx@wzmc.edu.cn

Received date: April 15, 2018; **Accepted date:** April 23, 2018; **Published date:** May 01, 2018

Abstract

Objective: The aim of this article was to assess the effect of phthalates on the activities of *CYP2C9* and *CYP2C19 in vitro*.

Methods: In this study, recombinant *CYP2C9*1* and *CYP2C19*1* microsomes were used to investigate the effects of phthalates and their metabolites on corresponding enzyme activities *in vitro*. 2-100 μM substrate of enzyme was incubated with series concentration of phthalates for 30 min at 37°C. The metabolic products were detected by ultra-high performance liquid chromatography (UPLC) and ultra-high performance liquid chromatography-mass spectrometry (UPLC-MS/MS) method.

Results: Dibutyl phthalate (DBP) potently inhibited *CYP2C9*1* with an activity inhibition rate of 67.3% and half-maximal inhibitory concentration (IC50) of 29.63 μmol·L^{-1}, but its metabolite monobutyl phthalate (MBP) had no significant effect on it. On the contrary, di (2-ethylhexyl) phthalate (DEHP) had no effect on *CYP2C9**1, but its metabolite monoethylhexyl phthalate (MEHP) significantly inhibited the enzyme activity with an activity inhibition rate of 90.6% and IC50 of 6.37 μmol·L^{-1}. With regards to *CYP2C19**1, DBP completely inhibited the enzyme activity with an activity inhibition rate of 100% and IC50 of 2.63 μmol·L^{-1}, but its metabolite MBP had no effect on it; DEHP and MEHP also inhibited the activity of *CYP2C19**1. Further investigation showed MEHP is a competitive inhibitor of *CYP2C9*1* (Ki=7.063 μmol·L^{-1}), and DBP is a competitive inhibitor of *CYP2C19*1* (Ki=7.013 μmol·L^{-1}) against their substrates, both phthalates are uncompetitive for the cofactor NADPH.

Conclusion: Our results suggested that DBP, DEHP and their metabolites exhibited potently inhibitory effects toward *CYP2C9*1* or *CYP2C19**1. And these findings provided valuable information for a potentially toxic mechanism of DEHP and DBP on endocrine disruption and a useful guidance for safe and effective usage of drugs in patients who have long-time DEHP and DBP exposure.

Keywords: Cytochrome P450 enzyme; Enzyme inhibition; Dibutyl phthalate; Monoethylhexyl phthalate; Metabolites; Phthalates

Introduction

Phthalates are used extensively as plasticizers. DBP and DEHP are high production volume plasticizers present in food products such as butter, infant formula and multiple vitamins, as well as in a variety of PVC and cosmetics [1-3]. The amount of DEHP and DBP in PVC may reach up to 40 ± 60% which can be detected in air, soil and aquatic ecosystems due to its continuous release into the environment [3,4]. DBP and DEHP can be taken by the general population from their diet, drinking water [5]. Toxicity and bioaccumulation of DBP and DEHP have raised a huge concern which are a serious threat to the environment and to human health. DBP and DEHP are predominantly metabolized into monobutyl phthalate (MBP) and mono-(2-ethylhexyl)-phthalate (MEHP), respectively [5]. Animal studies had confirmed that DBP, DEHP and corresponding metabolites were endocrine-disrupting chemicals [6] which might lead to reproductive disruption [7], such as an increase in testicular cancer and hypospadias as well as a decrease in sperm counts [6]. However, less is known about the effect of DBP, DEHP and their metabolites on drug metabolism mediated by cytochrome P450 (CYP).

CYPs are the most important drug-metabolizing enzymes, which are responsible for the metabolism of both endogenous and exogenous compounds in human body including steroids, drugs, and environmental pollutants, etc. [8-10]. Among all CYP isoforms in humans, *CYP2C9*1* and *CYP2C19*1* are the important enzymes responsible for metabolizing many of the drugs used in clinical practice [11]. *CYP2C9* makes about 20% CYP proteins in the human liver and responsible for the metabolism of approximately 20% clinically used drugs [11]. *CYP2C19*s expression level accounts for only 1% of the total CYP enzymes in the liver. However, it is involved in the metabolism of approximately 10% of the drugs used in clinical practice [11]. Therefore, detailed analysis of the *CYP2C9*1* and *CYP2C19*1* functional changes caused by DBP and DEHP and their metabolites should be facilitated to clarify their toxic mechanism. DBP and DEHP are well established to have an activity as endocrine disruptors [12,13]. However little attention has been given to the

possibility that they may also influence endocrine homeostasis *via* effects on CYP-mediated hormonal metabolism, and they may interact with clinically used drugs *via* inhibition of CYP activities. To evaluate the functional effects of CYP, *in vitro* studies using cDNA, expression systems have been proved to be the fastest and efficient tools in analyzing the drug metabolism in human with variant alleles of CYPs *in vivo* [14].

In this work, we addressed the major phthalates's effect on metabolism by measuring the inhibitory effects of DBP and DEHP, as well as their hydrolytic metabolites, on the activities of individual *CYP2C9* and *CYP2C19*, using series of specific substrates.

Materials and Methods

Materials

DBP, MBP, DEHP and MEHP (purity>98%) were purchased from AccuStandard, Inc. (New Haven, CT, USA). Diclofenac, 4'-hydroxy diclofenac (purity>98%), voriconazole and voriconazole N-Oxide (purity>98%) were purchased from Melone Biotechnology Co., Ltd. (Beijing, China). Phenacetin and fluconazole (purity>98%) were purchased from National Institute for the Control of Pharmaceutical and Biological Products (Beijing, China). The NADPH-regenerating system was obtained from Sigma-Aldrich (St. Louis, MO). Recombinant *CYP2C9*1* and *CYP2C19*1* microsomes and P450 cytochrome b5 were provided by Beijing Hospital (Beijing, China). An acquity ultra-performance liquid chromatography (UPLC) BEH C18 column (2.1 mm × 50 mm i.d., 1.7 μm particle size) was obtained from Waters (Dublin, Ireland). Ultrapure water was freshly purified by a Milli-Q A10 System (Millipore, Billerica, MA, USA). Other solvents and chemicals were of analytical grade as required.

Methods

Enzyme incubation procedure

The enzyme incubation mixtures contained the following: phosphate-buffered saline, *CYP2C9*1* or *CYP2C19*1* recombinant microsomes (5 pmol), purified cytochrome b5 (CYP/b5=1:1), 5uM substrate (diclofenac for *CYP2C9*1* and voriconazole for *CYP2C19*1*) and one of the inhibitors (DBP or MBP, DEHP or MEHP). After a 5-min preincubation in a shaking water bath (Shanghai Samsung Laboratory Instrument Co., Ltd. Shanghai, China), an NADPH regenerating system was added to start the reaction at 37°C in a final volume of 300 μL, and the mixture was incubated at the same temperature for 30 min. Reactions were terminated by cooling to -80°C for 15 min. Then 400 μL acetonitrile and 30 μL internal standards (35 μM diazepam for diclofenac, 16 μM fluconazole for voriconazole) were added to the tubes which was taken out of -80°C. After the vortex process, the incubation mixture was centrifuged at 13,000 rpm at 4°C for 10 min. The supernatant was diluted at 1:1 with ultrapure water, then 20 μL aliquot of the diluent was injected into the UPLC system for diclofenac analysis, and 2 μL aliquot of the diluent was injected into the UPLC-MS/MS system for voriconazole analysis. Incubations were performed in quadruplicate, the mean values ± SD from four experiments were provided for analysis.

Enzyme inhibition assays for *CYP2C9*1* and *CYP2C19*1*

Enzyme inhibition of DBP, MBP, DEHP and MEHP were assessed by detecting their effects on *CYP2C9*1* and *CYP2C19*1* activities. *CYP2C9*1* and *CYP2C19*1* activities were determined by diclofenac hydroxylation and voriconazole oxidation, respectively. Inhibition assays were performed as follows: Diclofenac (5 μM) was used as the common probe substrate for detecting *CYP2C9*1* activity. Voriconazole (5 μM) was used as the common probe substrate for detecting *CYP2C19*1* activity. The percent inhibitory effects of *CYP2C9*1* or *CYP2C19*1* activities, were measured in the presence of 100 μM inhibitor (DBP or MBP or DEHP or MEHP) in recombinant *CYP2C9*1* or *CYP2C19*1*, respectively. The percent inhibitory activity on *CYP2C9*1* or *CYP2C19*1* was calculated by the following formula

$$\text{Control activity}(\%) = \frac{(\text{Data of Test Group}/\text{Enzyme concentration})/\text{Incubation time}}{(\text{Data of Control Group}/\text{Enzyme concentration})/\text{Incubation time}}$$

Furthermore, the varying concentration (0.01, 0.1, 5.0, 10, 25, 50 and 100 μM) of each inhibitor (DBP or MBP or DEHP or MEHP) was respectively added to an incubation mixture to determine the half-maximal inhibitory concentration (IC50).

Inhibition modes assays of inhibitors

When the *CYP2C9*1* and *CYP2C19*1* were evidently inhibited by inhibitors, the inhibition modes of inhibitors were investigated further. In a separate study, a distinct final concentration of substrate (2.5, 5, 10, 25, 50, 100 μM) was incubated together with a reaction mixture containing 5 pmol recombinant *CYP2C9*1* or *CYP2C19*1* and 0-25 μM inhibitors to determine whether an inhibitor competes with diclofenac (the substrate of *CYP2C9*1*) or voriconazole (the substrate of *CYP2C19*1*). In another study, a different final concentration of NADPH (20, 50, 100, 200 μM) was incubated together with a reaction mixture containing 5 pmol recombinant *CYP2C9*1* or *CYP2C19*1* and 0-25 μM inhibitors to determine whether an inhibitor competes with the cofactor NADPH. Then, add 30 μL internal standards (35 μM diazepam or 16 μM fluconazole). After a series disposing similar with the above enzyme assay, the samples were measured by an UPLC or UPLC-MS/MS system. Kinetic studies were performed for determining the types of inhibition on CYP by the inhibitor.

Determination of 4'-hydroxydiclofenac by UPLC

UPLC system (Waters) was equipped with a quaternary pump, on-line vacuum de-gasser, auto sampler, thermostat controlled column compartment and UVD detector. The Waters ACQUITY BEH C18 column (50 mm 2.1 mm, i.d., 1.7 μm particle size) was maintained at 30°C and used for the separation of diclofenac, 4'-hydroxydiclofenac and diazepam. 276 nm was chosen as the detection wavelength. The mobile phase consisted of ultra-water (A)0.1% trifluoroacetate (B) and acetonitrile (C). We kept the flow rate at 0.4 mL/min and carried out a gradient elution program as follows: 0-1.5 min (50% A and 30% C), 1.5-2.5 min (50%–20% A and 30 %-60% C), 2.5-4.0 min (20% A and 60% C) and 4.0-4.3 min (20%-50% A and 60%-30% C). The total run time was 4.3 min.

Determination of voriconazole N-Oxide by UPLC-MS/MS

An Acquity UPLC system, which consisted of a solvent manager, a sample manager, a column and a Xevo TQD triple quadrupole mass spectrometer (Waters, Milford, MA), was used to analyze the samples. Compounds were separated using an Acquity UPLC BEH C18 column (2.1 mm 50 mm, 1.7 μm; Waters) and maintained at 40°C. The mobile phase consisted of acetonitrile (A) and 0.1% formic acid (B). We kept the flow rate at 0.4 ml/min and carried out a gradient elution program as follows: 0-0.5 min (25%-95% A), 0.5–1.7 min (95% A), 1.7–2.0 min

(25% A). The total run time was 2.5 min. Under the above conditions, voriconazole N-Oxide and fluconazole were well separated and their retention times were 1.35 min and 0.81 min, respectively. The Xevo TQD mass spectrometer was set to positive ion mode. Nitrogen served as the desolvation gas with flow rate of 1000 L/h and the desolvation temperature was maintained at 500°C. The temperature of the ionization source was kept at 150°C while the capillary voltage was set at 2000 V. Multiple reaction monitoring modes were as follows: mass-to-charge ratio (m/z) 307.1→238.1 and m/z 366.1→224.1 for fluconazole and voriconazole N-Oxide, respectively. The collision energy for fluconazole and voriconazole N-Oxide was both set at 15 V; the cone voltage for each was set at 35 V and 25 V, respectively (Table 1).

Drug	[M+H]+(m/z)	Cone voltage (V)	Mass transition (m/z to m/z)	Collision energy (V)
Voriconazole N-Oxide	366.1	25	366.1 → 224.1	15
Fluconazole (ISTD)	307.1	35	307.1 → 238.1	15

Table 1: Mass-to-charge (m/z) values for the protonated and fluconazole obtained by ESI+ and mass transitions used for quantification in the MRM mode.

Statistics

The percentage inhibition of phthalates was calculated to value the CYP activity by UPLC and UPLC–MS/MS. The IC50 value was calculated using GraphPad (version 5; GraphPad Software Inc., San Diego, CA, USA), and non-linear regression of a curve fit with one-site competition was performed. Lineweaver-Burk analysis was used to determine the mode of inhibition. The inhibition constant (Ki) was obtained by a secondary plot using the slopes of the primary Lineweaver-Burk Plot. αKi was obtained from a secondary plot using the y-intercepts of the Lineweaver-Burk plot. All results were analyzed in quadruplicate. One-way analysis of variances was used to estimate the significance of differences. All data were expressed as means ± SD. There was statistical significance between control and test groups if was $p<0.05$.

Results

Chromatographic analysis

Use chromatographic analysis to assess catalytic activity of *CYP2C9*1* and *CYP2C19*1 in vitro*. Under the above chromatographic conditions, we separated the metabolites and IS after incubation. Typical chromatograms of standard sample spiked with 4'-hydroxydiclofenac and diazepam (IS), and an incubation sample of *CYP2C9*1* recombinant microsome are shown in (Figures 1A and 1B). 4'-Hydroxydiclofenac and diazepam were well separated and their retention times were 2.98 and 0.80 min, respectively. The UPLC-MS/MS mass spectrogram and chromatogram of voriconazole N-Oxide and fluconazole (IS) which contain the *CYP2C19*1* incubated samples are presented in (Figures 2A and 2B). Voriconazole N-Oxide and fluconazole's retention times were 1.35 and 0.81 min, respectively.

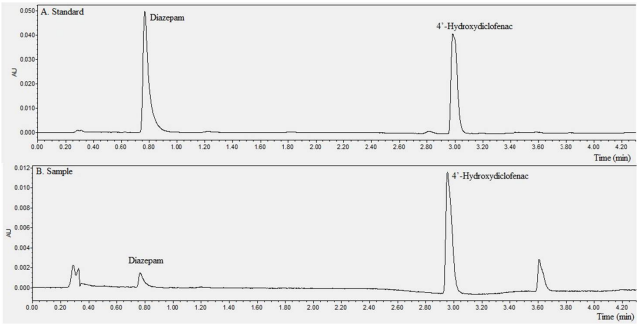

Figure 1: UPLC chromatograms of 4'-hydroxydiclofenac and diazepam. (A) Representative chromatograms for a standard sample spiked with 4'-hydroxydiclofenac and diazepam. (B) Representative chromatograms for an incubation sample of *CYP2C9*1* recombinant microsome.

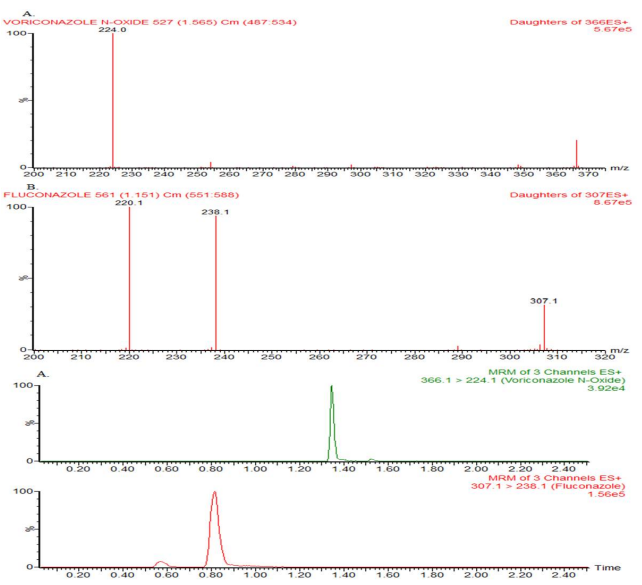

Figure 2: UPLC–MS/MS analysis of voriconazole N-Oxide and fluconazole. (A) Representative mass spectrogram for voriconazole N-Oxide. (B) Representative mass spectrogram for fluconazole. Representative chromatograms for voriconazole N-Oxide and fluconazole in an incubation sample of *CYP2C19*1* recombinant microsome.

Effects of DBP and MBP or DEHP and MEHP on *CYP2C9*1*

When maximum concentration of inhibitor (DBP, MBP, DEHP or MEHP, 100 μM) was used, DBP, MBP, DEHP and MEHP inhibited *CYP2C9*1*-catalyzed 4'-hydroxydiclofenac with 67.71%, 1.34%, 17.04% and 90.68%, respectively (Figures 3A and 3B). These data verified that DBP and MEHP exhibited potently inhibitory effects on *CYP2C9*1*. Further research is to be found that DBP and MEHP inhibit *CYP2C9*1* at a concentration-dependent manner in the presence of a range of concentrations (0.01, 0.1, 5, 10, 25, 50, 100 μM) of inhibitors DBP and MEHP (Figures 4A and 4B). Meanwhile these data indicated

that IC50 values of DBP and MEHP on *CYP2C9*1* were 29.63 μM and 6.365 μM, respectively (Figures 4C and 4D).

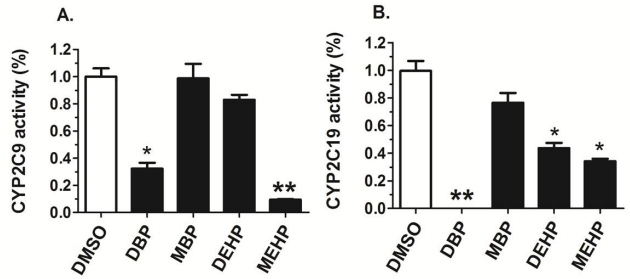

Figure 3: Inhibitory potential of DBP, MBP, DEHP and MEHP on *CYP2C9* (A) and *CYP2C19* activity (B). $^{*}P < 0.05$; $^{**}P < 0.01$ in comparison with the control.

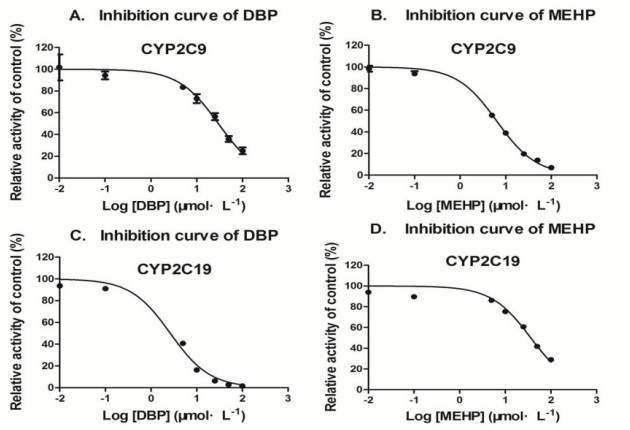

Figure 4: Inhibition of *CYP2C9* and *CYP2C19* by DBP and MEHP. (A) The remaining enzyme activities of recombinant *CYP2C9* in the presence of a range of concentrations (0.01, 0.1, 5, 10, 25, 50, 100 μM) of DBP were determined by measuring the formation rates from . (B) The remaining enzyme activities of recombinant *CYP2C9* in the presence of a range of concentrations (0.01, 0.1, 5, 10, 25, 50, 100 μM) of MEHP were determined by measuring the formation rates from . (C) The remaining enzyme activities of recombinant *CYP2C19* in the presence of a range of concentrations (0.01, 0.1, 5, 10, 25, 50, 100 μM) of DBP were determined by measuring the formation rates from . (D) The remaining enzyme activities of recombinant *CYP2C19* in the presence of a range of concentrations (0.01, 0.1, 5, 10, 25, 50, 100 μM) of MEHP were determined by measuring the formation rates from . Each data point represents the mean of quadruplicate determinations.

Mechanism of inhibition of *CYP2C9*1* by MEHP

Due to MEHP evidently inhibited the activity of *CYP2C9*1* in a concentration-dependent manner, using MEHP to further determine the mode of *CYP2C9*1* inhibition. Enzyme kinetics studies were carried out with various substrates concentrations in the presence or absence of MEHP [15]. Lineweaver–Burk transformation of the enzyme velocities versus substrates concentrations showed that the lines for each MEHP concentration crossed on the left of the Y-axis (Figure 5A), indicating that MEHP acts on *CYP2C9*1* activity as a competitive inhibitor when using diclofenac as a substrate. To calculate Ki and α, the slope and the intercept of the Lineweaver–Burk lines for concentrations of MEHP as an inhibitor were plotted as a function of inhibitor concentration (Figure 5B). The intersections of the lines from slope and intercept with the X-axis show Ki (7.036 μmol·L^{-1}) and αKi (42.68 μmol·L^{-1}), respectively. Furthermore, when NADPH was investigated, the Lineweaver–Burk plots analysis showed that the mode of inhibition by MEHP for *CYP2C9*1* was uncompetitive inhibition against NADPH (Figure 5C).

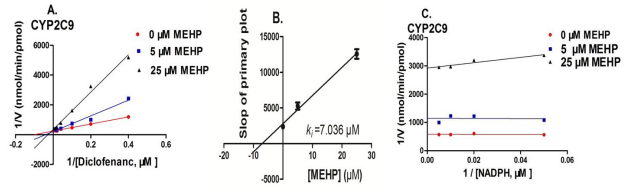

Figure 5: Lineweaver-Burk plots of *CYP2C9* activity in the presence of MEHP. (A) *CYP2C9* activity was measured by the velocity of diclofenanc to diclofenac 4'-hydroxylation in *CYP2C9* microsomal protein for 30 min in the presence of varying concentrations of the substrate diclofenanc (2.5, 5, 10, 25, 50 and 100 μM). (B) The secondary Lineweaver–Burk plot for Ki in the inhibition of *CYP2C9*-mediated diclofenanc metabolism by various concentrations of MEHP (0, 5, 25 μM) in recombinant *CYP2C9* microsomes. (C) *CYP2C9* activity was measured by the velocity of diclofenanc to diclofenac 4'-hydroxylation in microsomal protein for 30 min in the presence of varying concentrations of the cofactor NADPH (20, 50, 100 and 200 μM). Each data point represents the mean of quadruplicate determinations.

Effects of DEHP or MEHP and DBP or MBP on *CYP2C19*1*

As shown in the Figure 3B, when the above plasticizers (100 μM) was separately used in the *CYP2C19** 1-catalyzed system, voriconazole N-Oxide was suppressed by 100.0%, 23.58% and 56.39%, 65.90% under the action of DBP, MBP, DEHP and MEHP respectively (Figures 6A and 6B). This data indicated that DBP and MEHP exhibited potently inhibitory effects on *CYP2C19** 1. Depending on the enzyme activities of recombinant *CYP2C19*1* in the presence of a range of concentrations (0.01, 0.1, 5, 10, 25, 50, 100 μM) of the above inhibitor, our results showed the DBP and MEHP inhibit *CYP2C19*1* at a concentration-dependent manner (Figure 6C). And the data showed the IC50 values of DBP and MEHP on *CYP2C19*1* were 2.639 and 36.22 μM.

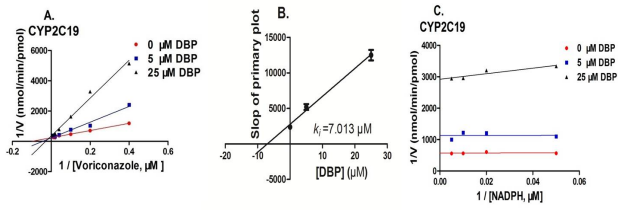

Figure 6: Lineweaver–Burk plots of *CYP2C19* activity in the presence of DBP. (A) *CYP2C19* activity was measured by the velocity of voriconazole to voriconazole N-Oxidein in *CYP2C19* microsomal protein for 30 min in the presence of varying concentrations of the substrate voriconazole (2.5, 5, 10, 25, 50 and 100 μM). (B) The secondary Lineweaver–Burk plot for Ki in the inhibition of *CYP2C19*-mediated voriconazole metabolism by various concentrations of DBP (0, 5, 25 μM) in recombinant *CYP2C19* microsomes. (C) *CYP2C19* activity was measured by the velocity of voriconazole to voriconazole N-Oxidein in microsomal protein for 30 min in the presence of varying concentrations of the cofactor NADPH (20, 50, 100 and 200 μM). Each data point represents the mean of quadruplicate determinations.

Mechanism of inhibition of *CYP2C19*1* by DBP

DBP obviously inhibited the activity of *CYP2C19*1* in a concentration-dependent manner. To further determine the mode of *CYP2C19*1* inhibition by DBP, enzyme kinetics studies were carried out with various substrates concentrations in the presence or absence of DBP [15]. Lineweaver–Burk transformation of the enzyme velocities versus substrates concentrations showed that the lines for each DBP concentration crossed on the left of the Y-axis (Figure 5A), indicating that DBP acts on *CYP2C19*1* activity as a competitive inhibitor when using voriconazole as a substrate. To calculate Ki and α, the slope and the intercept of the Lineweaver–Burk lines for concentrations of DBP as an inhibitor were plotted as a function of inhibitor concentration (Figure 5B). The intersections of the lines from slope and intercept with the X-axis show Ki (7.013 μmol·L^{-1}) and αKi (42.27 μmol·L^{-1}), respectively. Furthermore, when NADPH was investigated, the Lineweaver–Burk plots analysis showed that the mode of inhibition by DBP for *CYP2C19*1* was uncompetitive inhibition against NADPH (Figure 5C).

Discussion

DBP and DEHP were ones of the most important and ubiquitous environmental contaminants [12,16]. They can enter the human body through inhalation, ingestion and dermal absorption [16] which are a serious threat to the environment and to human health. They are easily hydrolyzed in humans, and the unchanged parent compounds and their metabolites also have been detected in human urine and tissues [5]. Because of little attention has been given to the plasticizers effects on CYP-mediated metabolism, and they may interact with clinically used drugs *via* inhibition of CYP activities, here we value the influence of DBP and DEHP and their metabolites on *CYP2C9*1* and *CYP2C19**1. The CYP induction or inhibition can alter many endogenous and exogenous compounds biotransformation and bioavailability.

In the present study, we found that DBP, DEHP or their metabolites appeared different inhibition on *CYP2C9*1* and *CYP2C19**1. DBP can directly inhibit the activity of *CYP2C9*1* with 67.71% inhibition ration, while its metabolite MBP almost had no effect. Oppositely, DEHP, for itself, less affected the activity of *CYP2C9**1, but the metabolite MEHP showed significantly suppression on *CYP2C9*1* with 90.68% inhibition ration. On the other hand, for *CYP2C19**1, DBP almost totally inhibited the activity of enzyme, but its metabolite MBP hardly influence the enzyme; DEHP and MEHP both showed obvious inhibition, especially MEHP. These findings implied that DBP maybe show potent mechanism of toxicity through mediating *CYP2C9*1* and *CYP2C19**1, but whose influence will markedly reduce after being metabolized to MBP. While DEHP entered the body and transformed into MEHP, then produced more potential risk on the metabolism of *CYP2C9*1* and *CYP2C19*1* than its parent compound. Based on widely using and long-term exposure of DBP and DEHP, the variation of activity of *CYP2C9*1* and *CYP2C19*1* increase the risk of endocrine-disrupting effects due to inhibition of hormonal metabolism, as well as affecting drug response, such as pharmacokinetics, therapeutic effects and onset of adverse reactions of drugs[17].

Upon further study of the isozyme inhibition pattern, our study indicated that MEHP was the competitive inhibitor for *CYP2C9*1* against its substrate and the Ki value was 7.036 μmol·L^{-1}. Alternatively, DBP was also found to be the competitive inhibitor for *CYP2C19*1* against its substrate, and the Ki value was 7.013 μmol·L^{-1}. These indicated that MEHP and DBP inhibited *CYP2C9*1* or *CYP2C19*1* by competing with the substrate in its enzyme binding site, which interfere with *CYP2C9*1* (*CYP2C19**1)-NADPH-P450 reductase complex. The binding affinity of MEHP and DBP to *CYP2C9*1* and *CYP2C19*1* was higher than that to NADPH, which might be attributed to the competitive inhibition type of MEHP and DBP against *CYP2C9*1* and *CYP2C19**1. Therefore, when the MEHP and DBP plasma concentrations were close to the IC50 and Ki values, determined in this study, they could quite probably decrease the activities of *CYP2C9*1* and *CYP2C19*1 in vivo*. In fact, the CYP-mediated metabolism including a number of drugs with narrow therapeutic ranges, which caused an increase in their serum concentration and toxicity through inhibiting the above CYP enzymes [18].

Because *CYP2C9*1* and *CYP2C19*1* are involved in the metabolism of estrogen[17], the inhibition of the above CYPs by DBP and MEHP may be a contributing factor to endocrine disruption which can cause many diseases such as hypospadias, cryptorchidism, adult testiculoma, carcinoma of prostate and breast carcinoma [19]. In this study, we demonstrated that concentrations as low as 5 μM of DBP and MEHP suppressed *CYP2C9*1* and *CYP2C19*1* activity. The results presented herein identify additional mechanisms of action of DBP and MEHP in affecting normal endocrine function. Meanwhile *CYP2C9*1* and *CYP2C19*1* are responsible for the metabolism of many clinical drugs including warfarin and clopidogrel, etc [11]. So prolonged DBP or DEHP exposure maybe increase the risk for complications of coagulation system after the long-term treatment of the above drugs. Therefore, the mechanism of this interaction between plasticizers and endogenous and exogenous compounds has to be confirmed through further studies which are relevant to public health.

Conclusion

In conclusion, the data in this study demonstrated that DBP, DEHP and their metabolites exhibited potently inhibitory effects toward *CYP2C9*1* or *CYP2C19**1. In particular, DBP and MEHP are competitive inhibitors of *CYP2C9*1* and *CYP2C19*1* against the substrates, but an uncompetitive inhibitor against NADPH. These results provided useful guidance for safe and effective usage of drugs in patients who are long-time exposure in DBP or DEHP. Therefore the potential drug interaction and toxic mechanism should be brought to attention.

Acknowledgements

The authors thank Ministry of Health Beijing Institute of Geriatrics members for advice and assistance. This work was supported by Wenzhou Science and Technology Bureau (grant numbers 2016Y0450).

Conflict of Interest

The authors declare that there is no conflict of interest.

Reference

1. Wu CF, Hsiung CA, Tsai HJ, Tsai YC, Hsieh HM, et al. (2018) Interaction of melamine and di-(2-ethylhexyl) phthalate exposure on markers of early renal damage in children: The 2011 Taiwan food scandal. Environ Pollut 235: 453-461.
2. Shen O, Wu W, Du G, Liu R, Yu L, et al. (2011) Thyroid disruption by Di-n-butyl phthalate (DBP) and mono-n-butyl phthalate (MBP) in Xenopus laevis. PLoS One 6: e19159.
3. Gao M, Qi Y, Song W, Xu H (2016) Effects of di-n-butyl phthalate and di (2-ethylhexyl) phthalate on the growth, photosynthesis, and chlorophyll fluorescence of wheat seedlings. Chemosphere 151: 76-83.
4. Erythropel HC, Maric M, Nicell JA, Leask RL, Yargeau V, et al. (2014) Leaching of the plasticizer di(2-ethylhexyl)phthalate (DEHP) from plastic containers and the question of human exposure. Appl Microbiol Biotechnol 98: 9967-9981.
5. Wittassek M, Angerer J (2008) Phthalates: metabolism and exposure. Int J Androl 31: 131-138.
6. Wen Y, Liu SD, Lei X, Ling YS, Luo Y, et al. (2015) Association of PAEs with Precocious Puberty in Children: A Systematic Review and Meta-Analysis. Int J Environ Res Public Health 12: 15254-15268.
7. Wolff MS, Teitelbaum SL, Pinney SM, Windham G, Liao L, et al. (2010) Investigation of relationships between urinary biomarkers of phytoestrogens, phthalates, and phenols and pubertal stages in girls. Environ Health Perspect 118: 1039-1046.
8. Gonzalez FJ, Lee YH (1996) Constitutive expression of hepatic cytochrome P450 genes. FASEB J 10: 1112-1117.
9. Girennavar B, Jayaprakasha GK, Patil BS (2007) Potent inhibition of human cytochrome P450 3A4, 2D6, and 2C9 isoenzymes by grapefruit juice and its furocoumarins. J Food Sci 72: 417-421.
10. Belic A, Temesvari M, Kohalmy K, Vrzal R, Dvorak Z, et al. (2009) Investigation of the CYP2C9 induction profile in human hepatocytes by combining experimental and modelling approaches. Curr Drug Metab 10: 1066-1074.
11. Hiratsuka M (2016) Genetic Polymorphisms and in Vitro Functional Characterization of CYP2C8, CYP2C9, and CYP2C19 Allelic Variants. Biol Pharm Bull 39: 1748-1759.
12. Chen X, Xu S, Tan T, Lee ST, Cheng SH, et al. (2014) Toxicity and estrogenic endocrine disrupting activity of phthalates and their mixtures. Int J Environ Res Public Health 11: 3156-3168.
13. Jiang JT, Xu HL, Zhu YP, Wood K, Li EH, et al. (2015) Reduced Fgf10/Fgfr2 and androgen receptor (AR) in anorectal malformations male rats induced by di-n-butyl phthalate (DBP): A study on the local and systemic toxicology of DBP. Toxicology 338: 77-85.
14. Hiratsuka M (2012) In vitro assessment of the allelic variants of cytochrome P450. Drug Metab Pharmacokinet 27: 68-84.
15. Chen A, Zhou X, Tang S, Liu M, Wang X, et al. (2016) Evaluation of the inhibition potential of plumbagin against cytochrome P450 using LC-MS/MS and cocktail approach. Sci Rep 6: 28482.
16. Huang XF, Li Y, Gu YH, Liu M, Xu Y, et al. (2012) The effects of Di-(2-ethylhexyl)-phthalate exposure on fertilization and embryonic development in vitro and testicular genomic mutation in vivo. PLoS One 7: e50465.
17. Cheng ZN, Shu Y, Liu ZQ, Wang LS, Ou-Yang DS, et al. (2001) Role of cytochrome P450 in estradiol metabolism in vitro. Acta Pharmacol Sin 22: 148-154.
18. Ohno Y (2018) Quantitative Prediction of Drug-Drug Interaction Caused by CYP Inhibition and Induction from In Vivo Data and Its Application in Daily Clinical Practices-Proposal for the Pharmacokinetic Interaction Significance Classification System (PISCS). Yakugaku Zasshi 138: 337-345.
19. Sharpe RM (2003) The 'oestrogen hypothesis'- where do we stand now?. Int J Androl 26: 2-15.